Conformational Analysis of Cellulose Tripropionate

Yuichiro SHUTOH, Keizo OKAMURA, Fumio TANAKA
and Misato NORIMOTO

セルローストリプロピオネートの コンフォーメーション解析

首藤勇一郎・岡村　圭造・田中　文男・則元　　京

Résumé

The conformation of single cellulose tripropionate chain was studied by the virtual bond method considering nonbonded repulsive energy within the residue and between the contiguous residues. From X-ray data, the fiber repeat distance was found to be 1.508nm with systematic absences of threefold screw axis along the molecule. This threefold helical symmetry of cellulose tripropionate is unique among cellulose triester homologues in which the twofold screw axis is predominant. Considering 16 most probable conformations, 8 in right-handed and 8 in left-handed helical conformations, a left-handed 3_2 helical conformation was most favorable based on conformation analysis and short contact examinations between any pair of nonbonded atoms. The propionyl side chains are considerably extended almost perpendicularly to the helix axis.

要　　旨

セルローストリプロピオネート（CTP）の1本の分子鎖について，1残基内および連続する残基間の非結合原子間反発エネルギーを考慮したバーチュアルボンド法により，コンフォーメーション解析を行なった。X線繊維図から，CTP の繊維周期は1.508nm と計算され，消滅則より分子鎖方向に3回らせん軸が存在する。このように分子軸方向に3回らせん軸をもつセルローストリプロピオネートの構造は，他のセルローストリエステル同族体（セルローストリアセテート，セルローストリブチレート，セルローストリバレレート）が2回らせん構造を有するのに対して，特異的である。エネルギー計算および非結合原子間の容認されることのできない接触の有無を調べた結果，右巻き 3_1 らせんに比べ，左巻き 3_2 らせんの方が低いコンフォーメーションエネルギーを持つ事がわかった。考慮した16のモデルのうち，最も可能性の高い左巻き 3_2 らせんのコン

フォーメーションにおいては，側鎖はらせん軸に対しほぼ垂直に伸びた構造を持つ。

1. Introduction

The molecular and crystal structure of cellulose have been extensively studied by Sarko *et al*[1-4] in Syracuse and Blackwell[5,6] in Cleveland, and the conformation of cellulose molecule and the packing of neighboring chain were well established.

Among the aliphatic cellulose ester homologues the conformation was determined only of cellulose triacetate by Stipanovic and Sarko[7], and Roche *et al*[8]. The conformational analysis of higher ester homologues becomes very difficult, because, when one esterifies cellulose with higher aliphatic acid, conformational position of side group atoms varies independently and yet enormously different ways which needs formidably long computer time even with a most advanced computer.

In this study the conformation of cellulose tripropionate (CTP) molecule was determined based on X-ray data and conformational analysis of single molecule.

2. Experimental

2.1 Preparation of CTP

CTP was prepared by esterifying a purified ramie fiber in the mixture of trifluoroacetic anhydride and propionic acid. From proton nmr analysis, the ramie fiber was almost fully esterified (degree of substitution : 2.9).

A well-oriented CTP film was obtained by stretching in an oil bath at 140℃ to achieve maximal draw ratio (350%). The oriented film was further annealed in the oil bath at 180℃ to improve sharpness of CTP diffraction spots.

2.2 X-ray measurement

The X-ray fiber pattern was recorded in a flat film camera using nickel filtered Cu-Kα radiation.

3. Results and Discussion

3.1 X-ray structure of CTP

The X-ray fiber pattern of the oriented CTP film annealed in the oil bath at 180℃ is shown in Fig. 1. From the all of the layer line diffractions other than equatorial the fiber repeat was found to be 1.508nm. Since the virtual bond length of glucopyranose residue, the vector linking successive glycosidic bridge oxygens, is 0.544nm and the fiber diagram shows a systematic absence of (001) and (002) reflections, one can assume that there exists a threefold screw axis along the molecular direction. The systematic absence of (001) and (002) reflections were further confirmed by tilting the oriented CTP film by appropriate degrees. The advance per residue along the helix axis, h value, becomes 0.503nm considering that a threefold screw axis is present along the molecular axis. This value is considerably shorter than those of cellulose (h=0.515nm) as well as cellulose triacetate

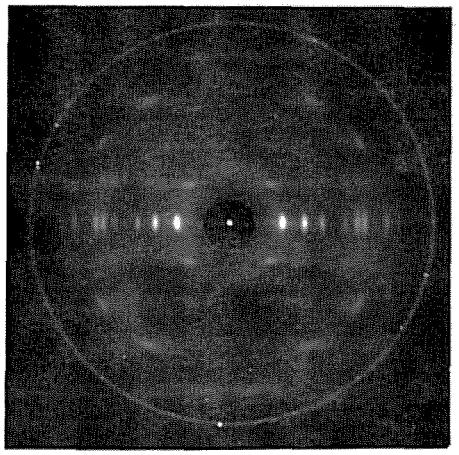

Fig. 1 X-ray fiber pattern of cellulose tripropionate annealed in an oil bath at 180℃. The Debye-Scherrer ring of (111) plane of CaF_2 was used for calibration purpose.

(h=0.525 nm) indicating CTP has a gentler slope.

3.2 Molecular model of CTP

From the X-ray data it was found that a threefold screw axis was present along the fiber axis, and the crystallographic asymmetric unit was the tripropionyl anhydroglucose residue. Once the first residue is transformed along the locus of the helix, the contiguous residues around the helix axis are easily generated by the helix symmetry operation.

3.2.1 The description of the residue

The description of the initial tripropionyl anhydroglucose residue of CTP is shown in Fig. 2, in which the virtual bond length between contiguous glycosidic oxygens, V. B., is represented by the dot-and-dashed lines. Initial values of the bond lengths (r_i), the bond angles (θ_i) and the conformational angles (ϕ_i) were obtained from the atomic coordinates of the middle residue of cellotriose undecaacetate[9].

The glucose residue of cellulose molecule is "rigid", except for the atomic positions of hydroxymethyl O(6), and the virtual bond length of any of cellulose derivatives as well as cellulose has the value of 0.544nm. Figure 3 shows the relationships between the virtual bond length, L, and other helix parameters, in which h, μ' and Δ are the advance per residue along the helix axis, the slope of the pitch and the angle of turn per residue, respectively. The values h, l and R are expressed in terms of L and μ', and they are $L\cdot\sin\mu'$, $L\cdot\cos\mu'$, and $\frac{L}{2}\cdot\cos\mu'\cdot\mathrm{cosec}\left(\frac{\Delta}{2}\right)$, respectively, and Δ is $2\pi t/n$, where t is

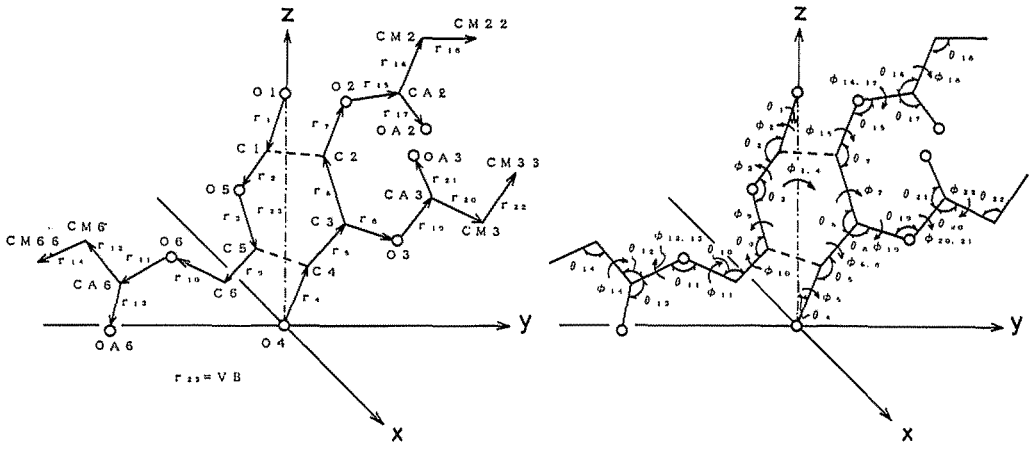

Fig. 2 Bond lengths (r_i), bond angles (θ_i), and conformational angles (ϕ_i) required for description of the residue. Hydrogen atoms are not shown.

number of turns in repeat and n is number of residues per repeat. In CTP h, t, n and Δ values have been determined to be 0.503 nm, 1, 3 and $\frac{2}{3}\pi$ from X-ray diagram, and considering the virtual bond value, L, is always equal to 0.544nm, and other values l, R and μ' become 0.207nm, 0.120nm and 67.6° respectively for the bridge oxygens. Among these values h and Δ are the same for any of the atoms in one residue to the corresponding atom of the contiguous residue.

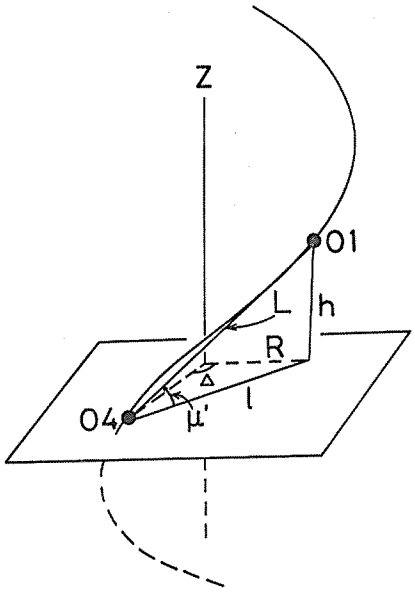

Fig. 3 A diagram showing relationship between virtual bond length and helix axis.

Once these parameters are fixed, together with the fixed bond lengths, bond angles and conformational angles, any atomic positions of one residue can be transformed to the contiguous residues until the helix completes the turn. Figures 4(a) and (b) show how the contiguous residues are generated from the starting residue along the right-handed 3_1, and left-handed 3_2 helices, respectively. The glycosidic bond angle, τ, varies as the angle θ rotates, which represents rotation of the entire glycosidic residue around the virtual bond (VB). Thus, by rotating the θ angle, one can build up all the possible chain conformations keeping threefold helix axis along the chain[10].

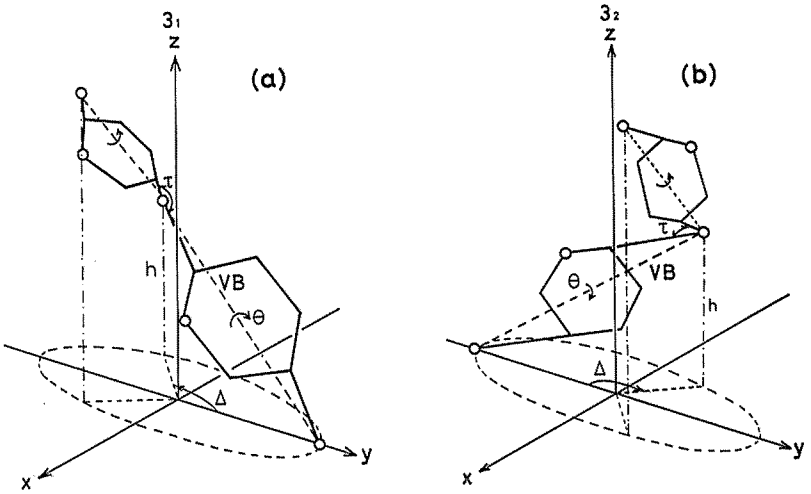

Fig. 4 Virtual bond length (VB) of residue and helix parameters (number of residues per turn of helix, n, and advance of residue along the fiber axis, h) determine positions of atoms in the contiguous residue($\Delta=2\pi/n$). Rotational angle of the residue around VB (θ) changes glycosidic bond angle, τ.

3.2.2 Conformation of the propionyl side chains

With respect to propionyl side chains, conformations of O(6) propionyl group were varied. Four possible rotational positions (gg, gt, tg, and gg + 180°) are shown in Fig. 5. Furthermore in each conformation, cis and trans conformations for CM(6) with respect to C(6) were considered (Fig. 6). This is legitimate since all the atoms in O(6)—CA(6)—CM(6) lie in one plane which is the case in polypeptides. OA(6)

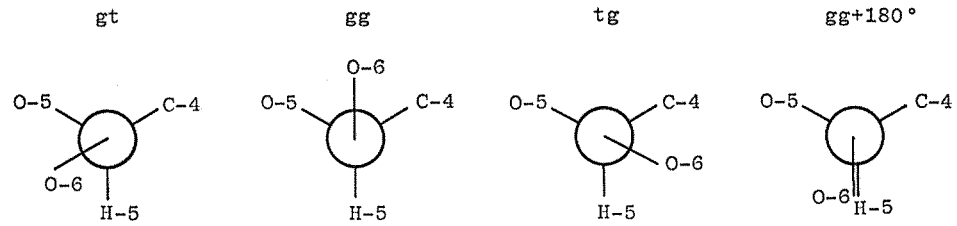

Fig. 5 Four probable positions of O(6) atoms with respect to O(5) and C(4): gt, gg, tg and gg+180°.

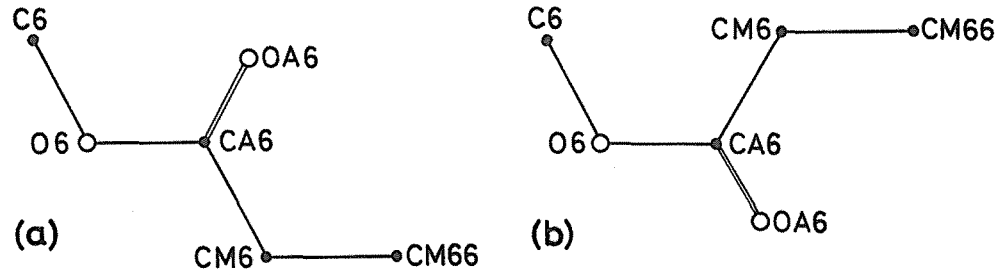

Fig. 6 Two probable conformations of CM(6) with respect to C(6): (a) trans, and (b) cis.

Finally the glycosidic bond angle τ was varied from 113° to 123°. Within this angle range the minimum conformational energy was sought for various conformational positions.

3.3 Calculations of nonbonded repulsive energy of isolated CTP chain

For the various conformations thus considered the nonbonded repulsive energy was calculated within one residue and/or between contiguous residues. The following quadratic nonbonded interatomic potential function (R_{pack}) proposed by Williams[11] was used for the calculation[12]:

$$R_{pack}=\sum_{\substack{i=1\\ j=1}}^{n} w_{ij}(d_{oij}-d_{ij})^2 \qquad (1)$$

where d_{oij} is nonbonded equilibrium distance between atoms i and j; d_{ij} is actual nonbonded distance between atoms i and j: w_{ij} is weighting factor for each interaction type; n is number of nonbonded contacts. The constants for each pair of atoms are given in Table 1[13].

Typical virtual bond angle *vs* energy plots for the right-handed and the left-handed CTP chains are given in Figs. 7(a) and 8(a), respectively. Within probable virtual bond angle range, the rotations around C(1)-O(1), Φ, and O(1)-C(4′), Ψ, as well as the glycosidic bond

angle (τ) were plotted against to the virtual bond angle [Figs. 7(b) and 8(b)].

In Fig. 7, in which the values were plotted against the virtual bond angle for a conformation of a right-handed CTP [O(6), gg+180°; CM(6), trans], the energy minimum was seen at $\theta=30°$. The corresponding τ angle was 123.7° which is too large to accept as the bridge angle for any carbohydrate compounds which ranges between 113° and 118°[14]. Besides, an unacceptable short contact was noticed between O(3) and H(1) atoms, which raised R_{pack} value, and this conformation was discarded. On the other hand, in Fig. 8, in which the values were plotted against the virtual bond angle for a conformation of a left-handed CTP [O(6), gt; CM(6), trans], the energy minimum was seen at $\theta=225°$, and the corresponding τ angle was 117.7° which is in the range of the bridge angle for carbohydrate compounds. Furthermore, no short contact was noticed between any pair of atoms.

Table 1 Weighting factors for nonbonded repulsion term in Eq.(1) (for $d_{ij} > d_{0ij}$, w=0).

Interaction type	d_{0ij}, Å	w
C·····C	3.70	3.00
C·····O	3.60	3.00
C·····H	3.30	1.35
O·····O	3.60	3.00
O·····H	3.25	1.40
H·····H	3.20	0.50

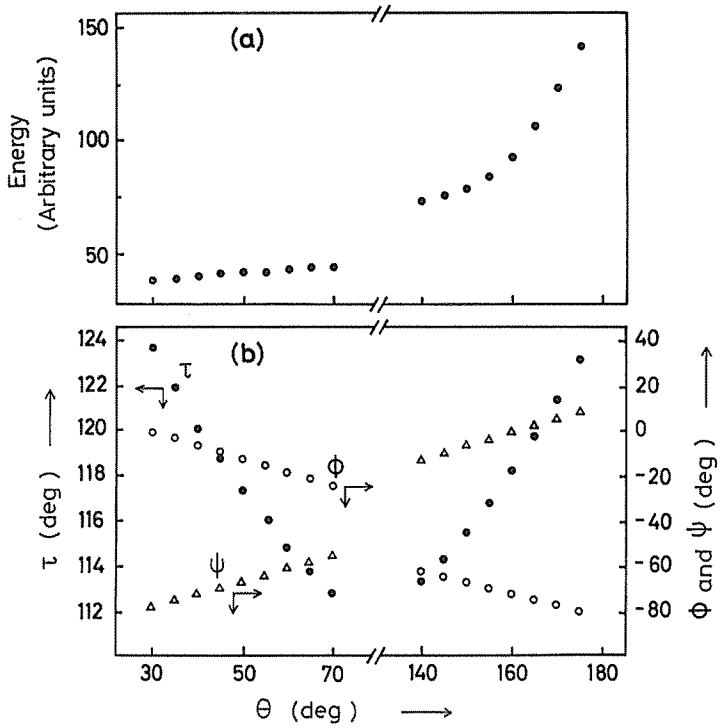

Fig. 7 Relationships between virtual bond rotation and conformational energy (a), and resulting τ, ϕ and ψ angles (b) for a right-handed CTP, where O(6) is gg + 180°, and CM(6) is trans positions.

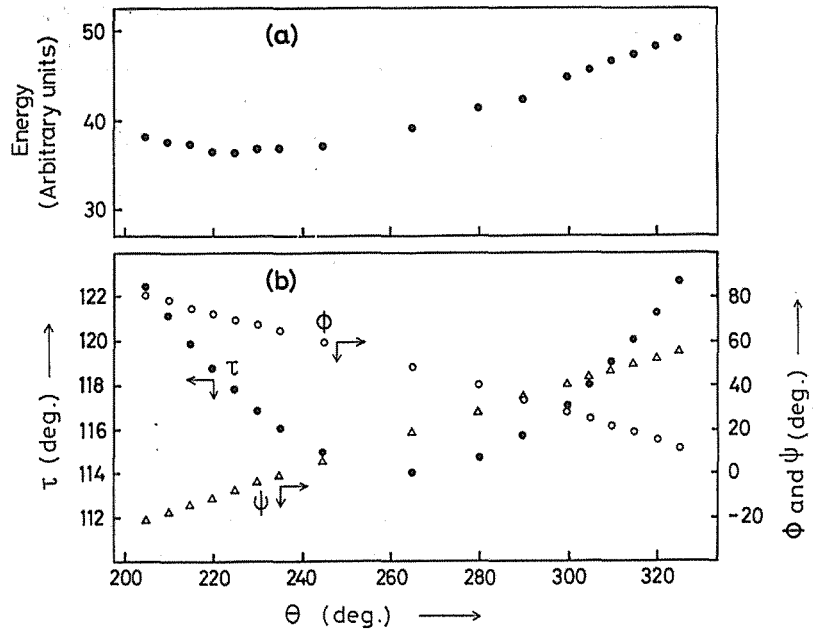

Fig. 8 Relationships between virtual bond rotation and conformational energy (a), and the resulting τ, ϕ and ψ angles (b) for a left-handed CTP, where O (6) is gt, and CM (6) is trans positions.

Table 2 Dependence of total repulsive energy, R_{pack}, for different models.

Models of CTP			R_{pack}	τ(°)	Φ(°)	Ψ(°)
helix	O6	CM6				
	gg	cis	42.543	121.9	-3.4	-75.6
		trans	41.449	121.9	-3.4	-75.6
3_1	gt	cis	41.911	123.7	-0.3	-78.3
		trans	39.130	123.7	-0.3	-78.3
right	tg	cis	42.705	123.7	-0.3	-78.3
handed		trans	40.738	123.7	-0.3	-78.3
	gg+180°	cis	40.210	123.7	-0.3	-78.3
		trans	38.501	123.7	-0.3	-78.3
	gg	cis	39.396	114.9	59.6	5.4
		trans	38.458	114.9	59.6	5.4
3_2	gt	cis	39.295	117.7	70.3	-7.9
		trans	36.279	117.7	70.3	-7.9
left	tg	cis	41.979	121.1	78.1	-18.1
handed		trans	44.130	122.5	80.8	-21.5
	gg+180°	cis	38.728	117.7	70.3	-7.9
		trans	37.048	117.7	70.3	-7.9

The minimum R_{pack} values for sixteen conformation models of CTP are listed in Table 2, eight for right-handed and eight for left-handed helices together with the resulting, Φ, Ψ and τ angles. For each helix four O(6) positions, and for each O(6), trans and cis CM(6) positions were considered. The R_{pack} values in the left-handed helix were lower except for the model of O(6) tg and CM(6) trans.

The lowest conformational energy among sixteen possible models was the left-handed 3_2 helix with O(6) gt and CM(6) trans, and R_{pack} value was 36.279. No short contact was noticed in this model, and we decided that this was the most probable chain conformation of CTP. The projections of all the atomic coordinates within one complete helix, one perpendicular and the other parallel to the helix, are shown in Fig. 9.

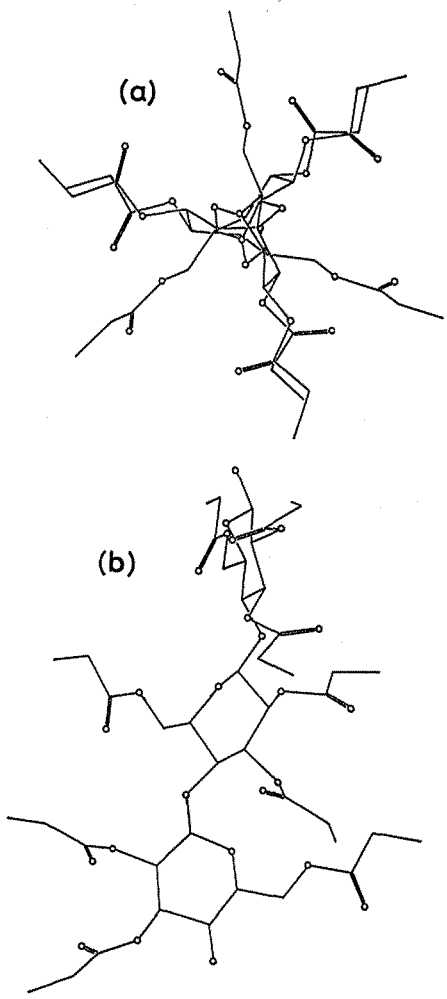

Fig. 9 Projections of the complete three residues of the left-handed 3_2 helix model of CTP, (a) x-y projection, and (b) y-z projection.

Acknowledgement

The authors express their sincere appreciation to Prof. Anatole Sarko, Department of Chemistry, State University of New York, College of Environmental Science and Forestry for his invaluable discussion and comment, and for the use of PS79 computer program. This work is supported by Scientific Research Grant No.60560176 (1985) of Ministry of Education, Science and Culture, which is greatly acknowledged.

4. References

1) SARKO, A. and MUGGLI, R.: Packing analysis of carbohydrates and polysaccharides. III. Valonia cellulose and cellulose II. Macromolecules. **7**. 486-494, 1974

2) WOODCOCK, C. and SARKO, A.: Packing analysis of carbohydrates and polysaccharides. 11. Molecular and crystal structure of native ramie cellulose. Macromolecules. **13**. 1183-1187, 1980

3) SARKO, A., SOUTHWICK, J. and HAYASHI, J.: Packing analysis of carbohydrates and polysaccharides. 7. Crystal structure of cellulose III_I and its relationship to other cellulose polymorphs. Macromolecules. **9**. 857-863, 1976

4) STIPANOVIC, A. J. and SARKO, A.: Packing analysis of carbohydrates and polysaccharides. 6. Molecular and crystal structure of regenerated cellulose II. Macromolecules. **9.** 851-857, 1976
5) GARDNER, K. H. and BLACKWELL, J.: The structure of native cellulose. Biopolymers. **13.** 1975-2001, 1974
6) KOLPAK, F. J. and BLACKWELL, J.: Determination of the structure of cellulose II. Macromolecules. **9.** 273-278, 1979
7) STIPANOVIC, A. J. and SARKO, A.: Molecular and crystal structure of cellulose triacetate I, a parallel chain structure. Polymer. **19.** 3-8, 1978
8) ROCHE, E., CHANZY, H., BOUDEULLE, M., MARCHESSAULT, R. H. and SUNDARARAJAN, P. R.: Three-dimensional crystalline structure of cellulose triacetate II. Macromolecules. **11.** 86-94, 1978
9) PEREZ, S. and BRISSE, F.: The crystal and molecular structure of a trisaccharide, β-cellotriose undecaacetate: 1,2,3,6-tetra-O-acetyl-4-O-[2,3,6-tri-O-acetyl-4-O-(2,3,4,6-tetra-O-acetyl-β-D-glucopyranosyl)-β-D-glucopyranosyl]-β-D-glucopyranose. Acta Cryst. **B33.** 2578-2584, 1977
10) SUNDARARAJAN, P. R. and MARCHESSAULT, R. H.: Virtual bond methods in conformational analysis of polymers. Can. J. Chem., **53.** 3563-3566, 1975
11) WILLIAMS, D. E.: A method of calculating molecular and crystal structures. Acta Cryst. **A25.** 464-470, 1969
12) ZUGENMAIER, P. and SARKO, A.: Packing analysis of carbohydrates and polysaccharides. I. Monosaccharides. Acta Cryst. **B28.** 3158-3166, 1972
13) ZUGENMAIER, P. and SARKO, A.: In "Fiber Diffraction Methods" (FRENCH, A. D. and GARDNER, K. C. H., ed). ACS Symposium Series No.141, American Chemical Society, Washington D. C. 225pp, 1980
14) SUNDARALINGAM, M.: Some aspects of stereochemistry and hydrogen bonding of carbohydrates related to polysaccharide conformations. Biopolymers. **6.** 189-213, 1968